JOURNAL OF AGRICULTURAL AND FOOD CHEMISTRY

Article

pubs.acs.org/JAFC

Identification of Early Fumonisin Biosynthetic Intermediates by Inactivation of the *FUM6* Gene in *Fusarium verticillioides*

Silvio Uhlig,*[,†] Mark Busman,[‡] Deborah S. Shane,[‡] Helene Rønning,[§] Frode Rise,[⊥] and Robert Proctor[‡]

[†]Norwegian Veterinary Institute, Ullevålsveien 68, 0454 Oslo, Norway

[‡]Agriculture Research Service, U.S. Department of Agriculture, Peoria, Illinois 61604, United States

[§]NorwegianSchool of Veterinary Science, P.O. Box 8146Dep, N-0033 Oslo, Norway

[⊥]Department of Chemistry, University of Oslo, P.O. Box 1033, Blindern, 0315 Oslo, Norway

ABSTRACT: Fumonisins are polyketide mycotoxins produced by the maize pathogen *Fusarium verticillioides* and are associated with multiple human and animal diseases. A fumonisin biosynthetic pathway has been proposed, but structures of early pathway intermediates have not been demonstrated. The *F. verticillioides FUM6* gene is required for an early pathway step. Here, metabolites produced by strains of the fungus with an inactivated *FUM6* gene were purified and shown by mass spectrometry and NMR spectroscopy to have fumonisin-like structures but without substitutions at C-14 and C-15. The major metabolite was 2-amino-12,16-dimethylicosane-3,10-diol. Lesser amounts of 3-keto and triol analogues of the metabolite were also identified. In precursor feeding experiments, 2-amino-12,16-dimethylicosane-3,10-diol was transformed to fumonisins by a *F. verticillioides* strain with an inactive fumonisin polyketide synthase gene. The results support the hypothesis that the *FUM6*-encoded enzyme catalyzes fumonisin C-14 and C-15 hydroxylation and provide direct spectroscopic and biochemical evidence for structures of early intermediates in fumonisin biosynthesis.

KEYWORDS: *biosynthesis, fumonisins, Fusarium verticillioides, mycotoxin, NMR*

INTRODUCTION

Fumonisins are a family of polyketide-derived mycotoxins that are produced by some species of the fungi *Aspergillus*, *Fusarium*, and *Tolypocladium* and can accumulate to high concentrations in maize infected with the fumonisin-producing species *Fusarium proliferatum* and *Fusraium verticillioides*.[1−3] Lower concentrations of fumonisins can also occur naturally in other crops, including rice, asparagus, grapes, and figs.[4−7] Fumonisins are of concern because they are epidemiologically associated with esophageal cancer and neural tube defects in some human populations, and they can cause several animal diseases, including cancer and neural tube defects in experimental rodents.[8,9]

In maize kernels, fumonisins B_1, B_2, B_3, and B_4 (**1**−**4**) are of greatest concern because they generally accumulate to higher concentrations than other fumonisin analogues (Figure 1). The structures of these B fumonisins include a linear 20-carbon chain substituted with an amine, two methyls, two tricarboxylate esters, and a C-3 hydroxyl.[10] The structures differ from one another by the presence and absence of hydroxyl functions at C-5 and C-10 (Figure 1). Enzymes that catalyze fumonisin biosynthetic reactions are encoded in the fumonisin biosynthetic gene (*FUM*) cluster. A biosynthetic pathway has been proposed based on the chemical structures of fumonisin analogues and the results of molecular and functional analyses of the *FUM* cluster genes in *F. verticillioides*.[11,12] The proposed pathway begins with the formation of 10,14-dimethyloctadecanoic acid, which then undergoes decarboxylative condensation with alanine to form 2-amino-12,16-dimethylicosane-3-one (Figure 2). Neither compound has been isolated or characterized from *Fusarium*; however, both are assumed to be part of the pathway based on structures of subsequent biosynthetic intermediates that have been characterized. In addition, 10,14-dimethyloctadecanoic acid may exist only as an enzyme-bound intermediate.[13] In the proposed pathway, 2-amino-12,16-dimethylicosane-3-one undergoes hydroxylation at C-14 and C-15 followed by esterification of six-carbon tricarboxylate moieties to the oxygen atoms at C-14 and C-15.[14] The resulting fumonisin analogue then undergoes reduction of the C-3 carbonyl to form a C-3 hydroxyl, as well as hydroxylation at C-5 and/or C-10 (Figure 2).

The functions of most *FUM* cluster-encoded enzymes in fumonisin biosynthesis have been elucidated by heterologous expression of the enzymes and/or inactivation of the corresponding genes.[11,12] In gene inactivation studies, *FUM* cluster genes were subjected to standard gene deletion or disruption strategies, and the resulting mutant strains were characterized for their ability to produce fumonisin analogues.[15,16] Precursor feeding studies with these analogues have provided evidence that at least some are fumonisin biosynthetic intermediates. To date, all fumonisin biosynthetic intermediates that have been purified and characterized structurally have oxygen atoms at C-14 and C-15. Strains of *F. verticillioides* in which the *FUM* cluster gene *FUM1*, *FUM6*, or *FUM8* has been inactivated (i.e., *fum1*, *fum6*, or *fum8* mutant) are of particular interest because no fumonisin biosynthetic intermediates have been purified from them

Received: July 10, 2012
Revised: September 18, 2012
Accepted: September 19, 2012
Published: September 19, 2012

dx.doi.org/10.1021/jf302967b | *J. Agric. Food Chem.* 2012, 60, 10293−10301

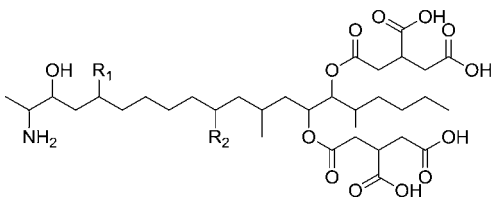

	R_1	R_2
1 Fumonisin B_1	OH	OH
2 Fumonisin B_2	OH	H
3 Fumonisin B_3	H	OH
4 Fumonisin B_4	H	H

Figure 1. Structures of fumonisins B_1–B_4 (**1**–**4**).

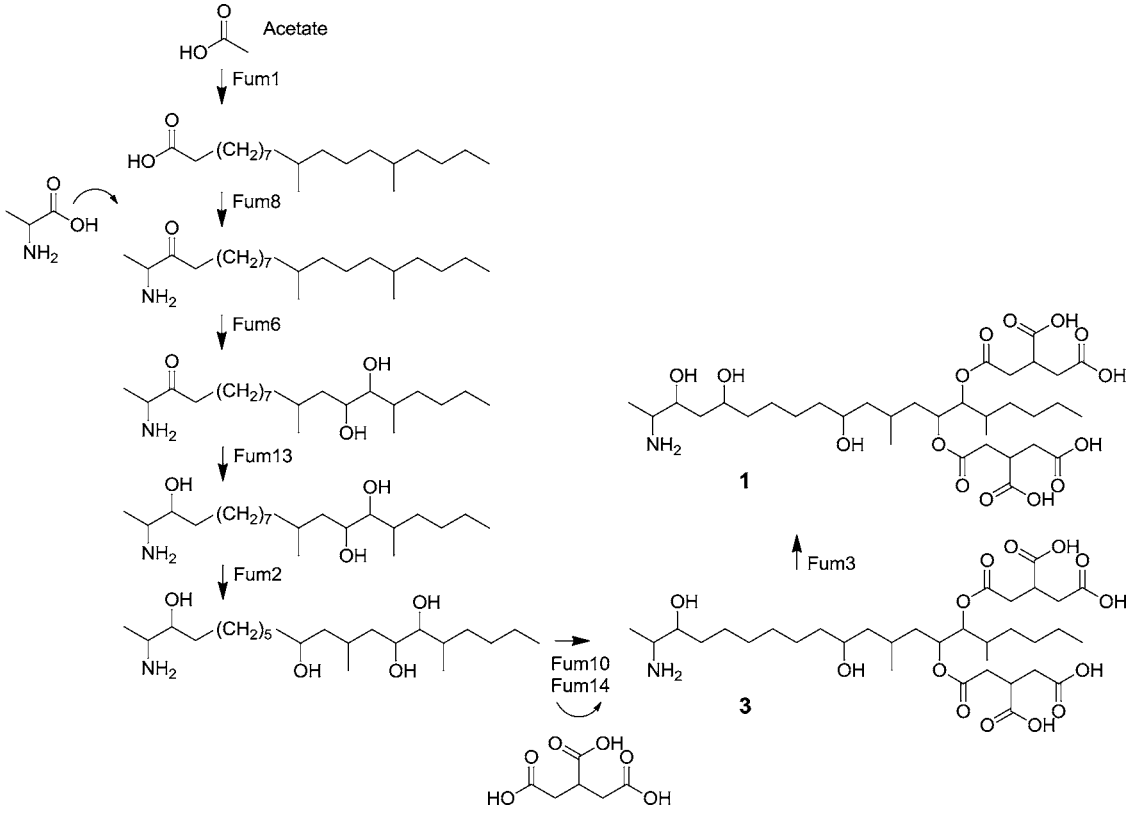

Figure 2. Proposed biosynthetic pathway for fumonisin B_1 showing functions of *FUM* genes/proteins.[11]

despite considerable effort.[14,17−19] This suggests that *FUM1*, *FUM6*, and *FUM8* are responsible for reactions that occur early in fumonisin biosynthesis, before C-14 and C-15 hydroxylation. This hypothesis is consistent with the predicted functions of the enzymes encoded by the genes. *FUM1* is predicted to encode a polyketide synthase that catalyzes the formation of a polyketide intermediate, 10,14-dimethyloctadecanoic acid, and *FUM8* is predicted to encode an oxoamine synthase that catalyzes the condensation of the polyketide and alanine to form the putative intermediate 2-amino-12,16-dimethylicosane-3-one.[12,13,18] The deduced amino acid sequence of *FUM6* is most similar to bifunctional cytochrome P450 monooxygenase-NADP reductases, enzymes that can catalyze hydroxylation reactions.[19] Given this and the inability of the *fum6* mutant to produce C-14 and C-15-hydroxylated fumonisin analogues, it is possible that the *FUM6*-encoded enzyme (Fum6) catalyzes fumonisin C-14 and C-15 hydroxylation.[14] When the *fum6* mutant was grown together with either the *fum1* or *fum8* mutant, the resulting culture produced several metabolites that were not detected in cultures of each mutant grown alone or in cultures of the fumonisin-producing progenitor strain.[14] Although mass spectrometric analysis suggested these metabolites had a linear fumonisin-like structure, further chemical characterization, including their purification and structure determination, was not performed. The objective of this study was to further elucidate the function of the Fum6 enzyme in fumonisin biosynthesis via re-examination of metabolites produced by *F. verticillioides fum6* mutants.

MATERIALS AND METHODS

Fungal Strains and Cultures. Gene and protein designations follow standard genetic nomenclature for *Fusarium*; for example, *FUM6* indicates a wild-type gene, *fum6* indicates a mutated gene, and Fum6 indicates a protein. Strains of *F. verticillioides* employed in this study have been previously described:[17,19] (1) the fumonisin-producing, wild-type strain FRC M-3125; (2) the fumonisin-nonproducing *fum6* mutant strains GfA3075 and GfA3080 that were generated from strain FRC M-3125 by partial deletion of the *FUM6* coding region; (3) strain GfA3151, which has a wild-type *FUM6* but carries the DNA plasmid used to generate *fum6* mutants as previously described;[19] and (4) the fumonisin-nonproducing *fum1* mutant strain GfA2364 that was generated by partial deletion of *FUM1* in strain FRC M-3125 as previously described.[17] For fumonisin production, strains were grown in 10 g of cracked maize kernel medium or in liquid GYAM medium as described previously.[19−21]

LC-MS-Based Metabolite Screening. Aliquots (1.0 g) of the freeze-dried cracked maize kernel cultures of *fum6* mutant and wild-type strains were homogenized with 7 mL of methanol for 1 min at

9500 min^{-1} (Ultra-Turrax T25, Janke& Kunkel, Staufen i. Br., Germany). The mixtures was then shaken on a multivortexer for 20 min (VWR International AS, Oslo, Norway) and centrifuged (200*g*, 30 min). Aliquots were filtered through 0.22 μm Spin-X Nylon filters (Costar, Corning, NY, USA) and then transferred to HPLC vials. The HPLC column was a 50 mm × 2.1 mm i.d., 3.5 μm, Symmetry Shield RP8 (Waters, Milford, MA, USA) fitted to a Finnigan Surveyor HPLC system equipped with an autosampler (Thermo Electron, San Jose, CA, USA). Elution was at 0.3 mL/min. Mobile phase A (pH 4.7) was prepared by dissolving 2.5 mM ammonium acetate in 10 mL of water, adding 2.5 mM glacial acetic acid, and then adding water to a final volume of 1 L. Mobile phase B was prepared with equal amounts of acid and base dissolved in 25 mL of water and then adding acetonitrile to a final volume of 1 L. Separation was performed using a gradient elution system that began with 3:1 mobile phase A/B and then changed to 100% B over 12 min. The column was flushed with mobile phase B for 2 min and then returned to 3:1 A/B for 2 min.

The HPLC was interfaced to a Finnigan LTQ linear ion trap mass spectrometer (ITMS, Thermo Electron), equipped with an electrospray ionization interface (ESI). The MS was run in the full-scan mode in the mass range m/z 200−800. Simultaneous fragmentation of the two most intense ions was achieved using data-dependent scanning. Ions above an intensity threshold of 10^4 were isolated with a 2 m/z unit isolation width; the activation *Q* was set to 0.25, and the activation time was set to 30 ms for fragmentation with a relative fragmentation energy of 35 units. The ESI, capillary voltage, and tube lens offset were optimized by continuous infusion of a 10 μg/mL solution of 2-amino-14,16-dimethyloctadecan-3-ol in methanol into a mobile phase composed of 1:1 A/B.

Isolation and Purification of Major Fumonisin-like Metabolites. Because LC-MS analysis indicated different *fum6* mutants exhibit similar metabolic profiles, freeze-dried cracked maize cultures of *fum6* mutant strains GfA3075 and GfA3080 were pooled to yield 20.9 g of raw material, which was homogenized (Ultra-Turrax T25, 9500 min^{-1}) in methanol for 10 min and then centrifuged for 10 min (12000*g*). The supernatant was filtered using S&S 595 folded filters (Schleicher & Schuell GmbH, Dassel, Germany) and the procedure repeated twice. Pooled supernatants were evaporated to dryness in a rotary evaporator to yield 1.7 g of a red-brown residue, which was dissolved in 80 mL of CH_2Cl_2/water (1:1) and then transferred to a separatory funnel. The evaporatory flask was successively rinsed with 80 and 60 mL of CH_2Cl_2/water (1:1) and transferred to the separatory funnel. The CH_2Cl_2 phase was collected and the water phase washed with 40 mL of CH_2Cl_2. Organic phases were combined and evaporated to yield 1.1 g of a red-brown oil. The oil was dissolved in 2 × 3 mL of CH_2Cl_2 and applied to a 400 mm × 20.0 mm i.d. glass column packed with 30 g of silica gel 60 (Fluka, Buchs, Switzerland). The column was eluted with a stepwise gradient (6 × 130 mL) composed of CH_2Cl_2 (F1), CH_2Cl_2/methanol (1:99, F2; 1:19, F3; 1:9, F4; 1:4, F5) and methanol/triethylamine (49:1, F6). Six fractions were collected according to mobile phase compositions. Metabolite **6** eluted primarily in F5, whereas all other metabolites (**5**, **7**, **8**, **9a**, and **9b**) eluted in F6. Fractions F5 and F6 were evaporated to dryness in a rotary evaporator to yield a solid brown residue of 0.1 g per fraction. Final purification was achieved using semipreparative HPLC. The column was a 250 mm × 10 mm i.d., 5 μm, Symmetry Shield RP8 (Waters) with a TSP model 4000 pump (Finnigan MAT Corp., now Thermo Fisher Scientific). The flow rate was 2.5 mL/min using a gradient solvent system that started with 40:60 methanol/water (both containing 0.1% of formic acid) and changed to 12:88 methanol/water over 20 min for separation of **5**, **7**, **8**, and **9a**,**b**. The column was flushed with methanol for 5 min and then returned to the starting conditions and re-equilibrated for 2 min. For final purification of **6**, the column was eluted with a gradient starting with 38:62 methanol/water (both containing 0.1% of formic acid) ramped to 28:72 methanol/water over 20 min. A portion of the eluent (approximately 10%) was continuously split into an LCQ Classic ITMS (Finnigan MAT Corp.) to guide the separation. The MS parameters were as follows: ESI positive mode; spray voltage, 4.5 kV; sheath gas flow rate, 60 arbitrary units; auxiliary gas flow rate, 5 arbitrary units; m/z range, 250−500. This procedure allowed for isolation and purification of approximately 1 mg of **7**, with submilligram amounts of **5**, **8**, and a mixture of **9a** and **9b** (estimated from NMR signal intensities).

HRMS of Semipure Metabolites. Aliquots from fractions of the silica gel cleanup were used to obtain HRMS data using an Agilent 6520 Accurate Mass Q-TOF mass spectrometer (Agilent Technologies, Inc., Santa Clara, CA, USA) equipped with an electrospray interface and coupled to an Agilent 1200 series HPLC pump and autosampler. HPLC conditions were identical to those described in the metabolite screening section. The parameters of the electrospray interface were set as follows: capillary voltage, 3.5 kV; drying gas flow, 5 L/min; gas temperature, 325 °C; nebulizer pressure, 30 psi. The Q/TOF mass spectrometer was scanned in the mass range m/z 100−1000 with a sampling rate of 1.4 spectra/s (4 GHz). The instrument was run with internal mass correction, and the fragmentor and skimmer voltages were set to 150 and 65 V, respectively.

NMR Spectroscopy. NMR spectra of compounds **7**, **8**, and a mixture of **9a** and **9b** were obtained from solutions (70 μL) in DMSO-d_6 (99.96 atom % D; Sigma-Aldrich) using 2.0 mm OD Norell tubes (Sigma-Aldrich) using a Bruker Match clamp holder (BrukerBioSpin, Silberstreifen, Germany). The spectra were acquired on an Avance AVI or AVII 600 MHz NMR spectrometer (BrukerBioSpin), both equipped with a 5 mm CP-TCI ($^1H/^{13}C$, $^{15}N-^2H$) triple-resonance inverse cryoprobe, equipped with a *Z*-gradient coil. NMR assignments (Table 2) were obtained from examination of ^1H, JMOD (compound **7** only), 1D-SELTOCSY, COSY, g-HSQC, g-HMBC, and H2BC (compound **7** only) NMR spectra. Additional HSQC-TOCSY spectra were obtained with d9s of 20 and 80 ms. The data were processed using Bruker TOPSPIN (version 1.3 or 2.1 pl4) software. Chemical shifts, determined at 25 °C, are reported relative to internal $CHD_2S(O)CD_3$ (2.49 ppm) and $CD_3S(O)CD_3$ (39.5 ppm).

Chemical Derivatizations; Acetylation and Methoxime Formation. The NMR sample containing a mixture of metabolites **9a** and **9b** was lyophilized and the residue dissolved in 1 mL of methanol. An aliquot (50 μL) was transferred to a 1.5 mL chromatography vial and evaporated. Pyridine (200 μL) and acetic anhydride (200 μL) were added to the vial, and the sample was left at room temperature overnight (18 h). Residual anhydride was destroyed by the addition of 400 μL of methanol and heating to 60 °C for 15 min. The sample was evaporated and the residue dissolved in 100 μL of acetonitrile. The sample was analyzed using LC-ITMS as outlined under LC-MS-Based Metabolite Screening with the following adjustments: a 100 × 2.1 mm Xbridge (3.5 μm) column (Waters) was used, the mobile phase gradient started at 1:1 A/B, and the ITMS was scanned in the mass range m/z 250−700.

An aliquot of the NMR sample of metabolite **6** was transferred to a 1.5 mL chromatography vial and lyophilized, and the residue was taken up in 200 μL of pyridine containing 1% of methoxyamine hydrochloride (Aldrich). The solution was placed at 40 °C overnight. The solvent was evaporated under N_2 at 60 °C, and the residue was dissolved in 200 μL of methanol. The sample was analyzed using LC-MS as outlined under LC-MS-Based Metabolite Screening with the following adjustments: a 50 × 2.1 mm Xbridge (2.5 μm) column (Waters) was used, and the ITMS was scanned in the mass range m/z 300−500.

Precursor Feeding Assays. For precursor feeding experiments, a 7 mm diameter agar plug, taken from the edge of a 7-day-old V-8 juice medium[20] culture, was placed in 150 mL of liquid GYAM medium and then incubated at 25 °C in the dark at 200 rpm for 4 days.[17]

Aliquots (20 or 200 μL) of compound **7** or **8**, suspended in methanol, were placed in the bottom of sterile 50 mL Erlenmeyer flasks. Flasks were left uncovered for 30−50 min in a biological safety cabinet to allow the methanol to evaporate. Twenty-milliliter aliquots of 4-day-old GYAM culture of the *fum1* mutant were placed in flasks containing either metabolite. The cultures were incubated at 25 °C in the dark at 200 rpm. Each metabolite feeding assay was done in triplicate. After 1 and 2 weeks of incubation, a 2.5 mL aliquot of each culture was filtered through a 0.2 μm cellulose acetate filter and then analyzed for the presence of fumonisins using the previously described LC-MS analysis.[22,23] In this analysis, the presence of **1**, **2**, and **3** was

determined by retention time and ESI spectra by comparison with purified standards of the metabolites.

RESULTS AND DISCUSSION

LC-MS and LC-MS^2 Metabolite Screening. The aim of this study was to verify the proposed function of the *F. verticillioides FUM6* gene in fumonisin biosynthesis. Initial LC-MS experiments were done to identify major fumonisin-like metabolites produced by *F. verticillioides fum6* mutants but not by their wild-type progenitor strain FRC M-3125. In these experiments, production of the wild-type complement of **1**−**4** was confirmed by LC-MS analysis of acetonitrile/water extracts of cracked maize cultures of the progenitor strain FRC M-3125. The absence of these fumonisin analogues in culture extracts of *fum6* mutant strains GfA3075 and GfA3080 was also confirmed by LC-MS analysis (data not shown).

The Fum6 enzyme is predicted to catalyze C-14 and C-15 hydroxylation of 2-amino-12,16-dimethylicosane-3-one, a metabolite that is predicted to result from condensation of alanine and a linear polyketide.[11,12,14] Thus, a possible consequence of *FUM6* gene deletion would be accumulation of 2-amino-12,16-dimethylicosane-3-one (molecular mass = 339 Da). A compound affording protonated molecular ions at m/z 340 was evident from the LC-MS chromatograms of extracts of cultures of the *fum6* mutants and likely corresponded to the 2-amino-12,16-dimethylicosane-3-one. The MS^2 spectrum of that compound supported this assumption as it was dominated by fragment ions due to water loss (−18 Da) as well as a series of hydrocarbon fragments (m/z 81/83/85 corresponding to $C_6H_9^+/C_6H_{11}^+/C_6H_{13}^+$, up to m/z 207 corresponding to $C_{15}H_{27}^+$) that are characteristic of the fumonisin backbone. The signal/noise ratio of the peak corresponding to the m/z 340 compound was, however, significantly lower than that of several other metabolites that yielded prominent peaks in the m/z 300−500 window and that shared the following mass spectrometric characteristics with the assumed 2-amino-12,16-dimethylicosane-3-one: (a) an odd molecular mass indicating the presence of a nitrogen atom, (b) cleavage of at least one molecule of water, and (c) a series of hydrocarbon fragments typically up to m/z 207 or 221 ($C_{15}H_{27}^+$ or $C_{16}H_{29}^+$) (data not shown). A peak eluting close to the m/z 340 compound, but with approximately 20 times higher signal intensity, afforded protonated molecular ions at m/z 342. The MS^2 fragment ion spectrum of the m/z 342 compound was similar to that of the m/z 340 compound (data not shown). The elemental composition of m/z 342 was determined to be $C_{22}H_{48}NO$ (Table 1), two hydrogen atoms more than a putative 2-amino-12,16-dimethylicosane-3-one, and is likely its 3-ol analogue, compound **5** (Figure 3).

Table 1. High-Resolution Mass Spectrometric Analyses for Fumonisin-like Metabolites 5−9 as Their Protonated Molecular Ions

		m/z		
metabolite	elemental composition	found	calcd	error (ppm)
5	$C_{22}H_{48}NO$	342.3735	342.3730	1.3
6	$C_{22}H_{46}NO_2$	356.3526	356.3523	0.8
7	$C_{22}H_{48}NO_2$	358.3693	358.3680	3.8
8	$C_{22}H_{48}NO_3$	374.3632	374.3629	0.9
9a,b	$C_{22}H_{48}NO_3$	374.3630	374.3629	0.3

Two compounds affording protonated molecular ions at m/z 356 and 358 dominated the m/z 300−500 window of the LC-MS chromatograms of the extracts of the *fum6* mutant cultures (Figure 4). Additionally, a cluster of three early-eluting compounds afforded protonated molecular ions at m/z 374 (Figure 4). Cleavage of up to three molecules of water (3 × 18 Da) upon fragmentation of the m/z 356, 358, and 374 compounds indicated hydroxylation of the molecules relative to 2-amino-12,16-dimethylicosane-3-one. Introduction of one and two oxygen atoms in the m/z 356/358 and 374 compounds, respectively, relative to 2-amino-12,16-dimethylicosane-3-one, was also well supported from their elemental composition obtained by HR-MS (Table 1). In addition, HR-MS verified that the mass difference between the m/z 356/358 pair of compounds corresponded to two hydrogen atoms.

Isolation and NMR Assignment. The procedure for the isolation of the putative fumonisin-like compounds from the *fum6* mutant cultures was based on that for the isolation of 2-amino-12,16-dimethyloctadecan-3-ol from cultures of *F. avenaceum*.[24] The procedure proved to be effective for the metabolites produced by the *fum6* mutants. However, even though the use of a silanol-shielded sorbent during final separation of fumonisin-like compounds was favorable for peak shape and resolution of individual compounds, baseline separation of the three m/z 374 compounds could not be achieved on a semipreparative scale.

The largest amount of high-purity (>98%) material was obtained for the m/z 358 compound (1−1.5 mg as assessed from the signal/noise ratio of NMR spectra). Detailed analyses of one-, two-, and three-dimensional NMR data including ^{1}H, JMOD, COSY, g-HSQC, g-HMBC, g-H2BC, HSQC-TOCSY, and SELTOCSY spectra determined in $(CD_3)_2S(O)$ identified this compound as 2-amino-12,16-dimethylicosane-3,10-diol (**7**) and afforded complete ^{1}H and ^{13}C assignments (Table 2). In accord with the HR-MS data, JMOD revealed the presence of 22 carbon resonances (4 methyl, 13 methylene, 5 methine). The two terminal methyl groups (H-1 at 1.02 ppm and H-20 at 0.85 ppm) were well resolved from other resonances and well suited as entry points for the NMR assignment. C-1 and C-2, which are predicted to be derived from alanine, were easily determined on the basis of correlations observed in the COSY, H2BC, and HMBC spectra.[14,25] Especially useful for the further assignment of the aliphatic chain to C-6 was the spectrum obtained from the H2BC experiment ($^2J_{H-CH}$ correlations) superimposed to a HSQC spectrum ($^1J_{H-CH}$ correlations), which allowed "walking" along the hydrocarbon backbone, whereas the COSY, HMBC, and HSQC-TOCSY spectra were used to support the structural information. As the NMR resonances for the methylenes at positions 6 and 7 were overlapping (^{1}H) or close (^{13}C), further assignment from that side of the chain was not possible. H-20 exhibited a well-resolved triplet in the ^{1}H spectrum at 0.85 ppm and was the obvious second entry point. This resonance showed correlations to H-19 in the COSY, H2BC, and HSQC-TOCSY (d9 = 20 ms) spectra, and $^2J_{H-CH}$−$^4J_{H-CH}$ coupling in the HMBC and HSQC-TOCSY (d9 = 80 ms) spectra (Figure 5). The H-16 methine proton showed correlations to two diastereotopic proton pairs at 1.03/1.22 and 1.05/1.25 ppm in the H2BC spectrum as well as to a methyl doublet at 0.82 ppm. Whereas the corresponding correlations between the H-16 methine and H-21 methyl protons were strong in the HSQC-TOCSY (d9 = 20 ms) and COSY spectra, the correlations between the H-16 and H-15/17 protons were weak and only noticeable for the

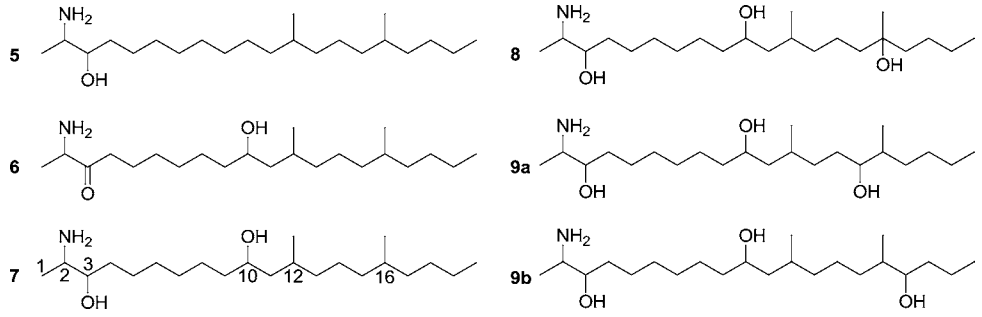

Figure 3. Structures of fumonisin-like metabolites produced by *fum6* mutants (strains GfA3075 and GfA3080) of *Fusarium verticillioides*. Structures for compounds **5** and **6** are tentative as NMR data were not available.

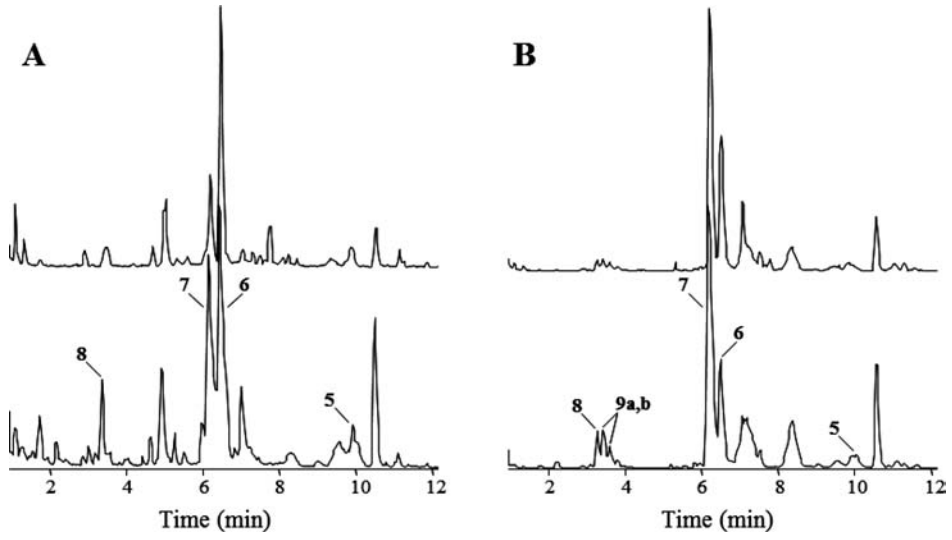

Figure 4. LC-MS chromatograms (m/z 250−450) of extracts from cracked corn cultures of two *fum6* mutants of *Fusarium verticillioides* (A) GfA3075 and (B) GfA3080 after incubation of cultures for 6 or 13 days (upper and lower traces, respectively).

1.03/1.05 ppm protons. Further C-/H-13 and C-/H-14 assignments were based on correlations observed in the H2BC, HSQC-TOCSY, and HMBC spectra. The C-9/H-9 to C-12/H-12 resonances of the hydrocarbon backbone were spread over a larger chemical shift range due to substitution at C-10 and C-12. The assignment of this part of the molecule was relatively straightforward by tracing the coupling environments of the COSY, HMBC, and H2BC spectra. H-12 (1.60 ppm) exhibited all possible correlations up to $^{3}J_{H-CH}$, that is, to C-10 and C-14 (Figure 5). The H2BC spectrum allowed extraction of the $^{2}J_{H-CH}$ coupling environment for H-12 and showed correlations to C-/H-22 (19.3/0.80 ppm), C-/H-13 (37.8/1.06, 1.17 ppm), and C-/H-11 (44.8/1.00, 1.28 ppm). Assignment of the C-/H-8 methylene was facilitated from the H2BC spectrum showing a clear correlation from C-9 to H-8, which was also observed in the HSQC-TOCSY (d9 = 20 ms) spectrum. Finally, the C-/H-8 methylene resonance was correlated in the HMBC, H2BC, and HSQC-TOCSY spectra to the poorly resolved methylene resonances at approximately 29.1/1.25 ppm (^{13}C/^{1}H), of which C-/H-6 was part. The hydroxyl- and amine-protons did not exhibit any visible ^{1}H resonance. However, it has been reported in the literature that especially the ^{1}H resonance of hydroxyls is often hidden below the water peak in DMSO-d_6.[26]

In our preliminary analysis of culture extracts of *fum6* mutants, the m/z 356 compound appeared to be present in amounts that were comparable to **7** (Figure 4). However, the m/z 356 compound was repeatedly lost during purification. Moreover, the signal intensity of the corresponding peak in culture extracts also decreased over time, indicating that this compound may be unstable. Therefore, we did not succeed in purifying sufficient material of this compound for NMR analysis. The LC-MS^2 and HR-MS data indicated that the m/z 356 compound is deficient in two hydrogen atoms relative to **7**, but possesses the same basic structure. To support the assumption that the m/z 356 compound could be the 3-one analogue of **7**, an aliquot of the sample originally destined for NMR was reacted with methoxyamine hydrochloride, which reacts with carbonyl groups to yield a methoxime derivative.[27] An overnight reaction of the m/z 356 compound yielded a product with a molecular mass 29 Da higher than the original mass and thereby confirmed the presence of a carbonyl group in m/z 356. We thus have good evidence for the m/z 356 compound being equivalent to 2-amino-10-hydroxy-12,16-dimethylicosane-3-one (**6**) (Figure 3).

The m/z 374 compounds were present in much lower quantities in culture extracts of the *F. verticillioides fum6* mutants, and the assignment of ^{1}H and ^{13}C resonances was therefore in part facilitated by comparison with the spectra obtained for **7**. Two separate m/z 374 isolates were obtained. For both m/z 374 isolates ^{1}H, COSY, g-HSQC, and g-HMBC spectra, as well as a set of HSQC-TOCSY (d9 = 20, 80, and 160 ms) and SELTOCSY (d9 = 20, 40, 80, and 160 ms) spectra, determined in $(CD_3)_2S(O)$, were successfully acquired.

Table 2. NMR Assignments for Major Fumonisin-like Metabolites (in DMSO-d_6) Produced by *fum6* Mutants of *Fusarium verticillioides*[a]

	7		8		9a		9b	
atom	^{1}H	^{13}C	^{1}H	^{13}C[b]	^{1}H	^{13}C[b]	^{1}H	^{13}C[b]
1	1.02 (d, J = 6.5 Hz)	13.0	0.96 (d, J = 6.4 Hz)	15.1	0.94 (d, J = 6.4 Hz)	15.8	0.94 (d, J = 6.4 Hz)	15.8
2	3.00	50.6	2.84	50.5	2.78	50.6	2.78	50.6
3	3.51	70.4	3.34	72.1	3.29	72.5	3.29	72.5
4	1.29	32.5	1.31	32.3	1.32	32.1	1.32	32.1
5	1.40	25.5	1.40	25.3	1.39	25.7	1.39	25.7
6	1.26	29.2[c]	1.22	28.9	1.22	29.3	1.22	29.3
7	1.26	29.1[c]	1.22	28.9	1.22	29.3	1.22	29.3
8	1.34	25.3	1.34	25.0	1.35	25.1	1.35	25.1
9	1.27	38.1	1.27	37.9	1.28	37.9	1.28	37.9
10	3.42	67.2	3.42	67.0	3.42	67.0	3.42	67.0
11	1.00; 1.28	44.8	1.00; 1.29	44.6	1.00; 1.29	44.6	1.00; 1.29	44.6
12	1.60	28.5	1.60	28.3	1.59	28.4	1.59	28.4
13	1.06; 1.17	37.8	1.07; 1.16	37.9	1.07; 1.18	37.6	1.07; 1.18	37.6
14	1.17; 1.29	23.8	1.22	25.4	1.16	30.5[d]	1.16	30.5[d]
15	1.03; 1.22	36.1	1.26	41.6	3.16	73.9	1.04; 1.23	36.6
16	1.32	32.0		70.5	1.38	38.1	1.35	31.7
17	1.05; 1.25	36.7	1.29	41.1	1.07; 1.25	36.2	3.42	72.2
18	1.18	28.7	1.22	25.4	1.13	28.9	[e]	[e]
19	1.24	22.4	1.23	22.6	1.25	22.5	1.25	22.5
20	0.85 (t, J = 6.7 Hz)	14.0	0.86 (t, J = 6.6 Hz)	13.9	0.85 (t, J = 7.0 Hz)	13.9	0.85 (t, J = 7.0 Hz)	13.9
21	0.82 (d, J = 6.2 Hz)	19.6	0.99 (s)	26.7	0.79 (d, J = 6.7 Hz)	15.2	0.82 (d, J = 6.4 Hz)	19.3
22	0.80 (d, J = 5.9 Hz)	19.3	0.81 (d, J = 6.4 Hz)	19.1	0.81 (d, J = 5.2 Hz)	19.3	0.81 (d, J = 5.2 Hz)	19.3

[a]Relative to internal $CHD_2S(O)CD_3$ at 2.49 ppm and $CD_3S(O)CD_3$ at 39.5 ppm. [b]Assignments based on g-HSQC and g-HMBC spectra. [c]Assignments interchangeable. [d]Uncertain assignment. [e]Not observed.

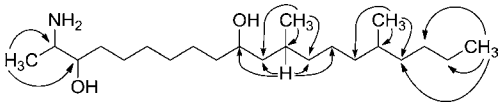

Figure 5. Key ^{1}H−^{13}C correlations observed in the HMBC NMR spectrum of 2-amino-12,16-dimethylicosane-3,10-diol (**7**).

Examination of the ^{1}H and HSQC spectra of the first m/z 374 compound revealed the following differences relative to the spectra of **7**: The methyl doublet observed at 0.82 ppm for **7** was shifted downfield (0.99 ppm) and appeared as a singlet; the methylene protons H-15 and H-17 did not appear as diastereotopic pairs (now at 1.29 and 1.26 ppm, respectively) and had moved to slightly higher ^{13}C chemical shift (41.1 and 41.6 ppm, respectively); the 16-methine resonance had disappeared from the spectra. These observations are consistent with hydroxylation of C-16 rendering the atom quaternary and thereby explain the methyl singlet at 0.99 ppm. Such a structural arrangement was further supported from the HMBC spectrum showing correlations from the 0.99 ppm methyl protons to a quaternary carbon at 70.5 ppm (i.e., no correlation in the g-HSQC) and to two methylene carbons at 41.1 and 41.6 ppm (C-15/17). The chemical shift of the quaternary carbon falls into the range expected for a hydroxylated carbon. Using a mixing time (d9) of 80 or 160 ms for acquisition of HSQC-TOCSY also revealed a correlation from the terminal H-20 at 0.86 ppm to a ^{13}C resonance at 41.1 ppm (C-17, $^4J_{H-CH}$) in addition to correlations to ^{13}C resonances at 25.4 ppm (C-18, $^3J_{H-CH}$), 22.6 ppm (C-19, $^2J_{H-CH}$), and 13.9 ppm (C-20, $^1J_{H-CH}$), whereas a mixing time (d9) of 20 ms gave correlations only up to $^2J_{H-CH}$ (C-19). H-15 was correlated in the HSQC-TOCSY spectrum (d9 = 20 ms) to a carbon at 25.5 ppm, likely belonging to C-14. All resonances from C-/H-4 to C-/H-13 as well as the C-/H-22 methyl group showed chemical shifts nearly identical to those of **7**. However, the chemical shifts of C/H-1−C/H-3 were affected by the hydroxylation 13−15 bonds away and had generally shifted to slightly lower ^{1}H chemical shifts (maximum −0.16 ppm for H-2) and slightly higher ^{13}C chemical shifts (maximum +2.2 ppm for C-1). This suggests folding of the chain such that the magnetic environment of the C-1 end of the molecule is influenced by the C-16 hydroxyl. In summary, the above data provide evidence that the first m/z 374 isolate is 2-amino-12,16-dimethylicosane-3,10,16-triol (**8**) (Figure 3).

The ^{1}H NMR spectrum of the second m/z 374 isolate exhibited three partly overlapping methyl doublets at approximately 0.80 ppm. However, the resonances belonging to the terminal methyl protons H-1 and H-20 appeared at about the same chemical shift as in **8**. The integral of the methyl doublets at ca. 0.80 ppm was approximately double the size of the integral for H-1 and H-20. Another interesting feature of the NMR spectra was the appearance of two resonances in the g-HSQC spectrum attributable to methine groups at a ^{1}H chemical shift similar to H-16 in **7** (1.35/1.38 vs 1.32 ppm in **7**) and at similar or slightly higher ^{13}C chemical shift compared to C-16 in **7** (31.7/38.1 vs 32.0 ppm in **7**). Four additional methine resonances appeared in the g-HSQC at ^{1}H/^{13}C chemical shifts of 3.42/67.0, 3.42/72.2, 3.29/72.5, and 3.16/73.9 ppm and are typical for resonances of hydroxylated methine groups. Reaction of a sample aliquot with acetic anhydride confirmed the presence of four acetylatable groups (one amine, three hydroxyls) by a molecular mass increase of 168 Da corresponding to 4 × $CH_3C(O)$ (data not shown). LC-ITMS chromatograms of the reaction mixture showed two baseline-separated peaks corresponding to the tetraacetylated derivatives of two isobaric analogues (data not shown).

Superimposition of the HSQC spectrum of the present sample with those of **7** and **8** suggested a structural difference at or close to C-16. This theory was at first complicated by the presence of methylene resonances in the HSQC spectrum of the second *m/z* 374 isolate at $^{1}H/^{13}C$ chemical shifts similar to C-/H-15 and C-/H-17 in **7**. One of the methyl doublets appeared at 0.79 ppm in the ^{1}H NMR spectrum and was thus relatively well separated from the other. This resonance was correlated to the methine proton at 1.38 ppm in the COSY spectrum. Because of its relatively good separation from other methyl resonances, it was possible to map out the coupling environment of the 0.79 ppm proton using a set of SELTOCSY (d9 = 20, 40, 80, 160 ms) and HSQC-TOCSY experiments (d9 = 20, 80 ms). Using a d9 of 20 ms, the SELTOCSY spectrum from irradiation of the 0.79 ppm doublet, subsequently identified as H-21, revealed correlations to the proton at 1.38 ppm (H-16) and to a proton at 1.07 ppm (H-17a). Increasing the d9 to 40 ms revealed additional correlations to a 1.25 ppm proton (H-17b) and to a proton at 3.16 ppm (H-15). Increasing the d9 further did not yield additional information because of signal overlap. However, using the SELTOCSY experiment and irradiation of the 0.85 ppm triplet (H-20) revealed a correlation to the 1.38 ppm methine proton (H-16, $^{6}J_{H-H}$) at d9 > 40 ms and to the 0.79 ppm doublet (H-21, $^{7}J_{H-H}$) at d9 > 80 ms. Correlations to the methine protons at 3.16 ppm were, however, not observed from H-20 using SELTOCSY. However, the methine proton at 3.16 ppm exhibited correlations in the COSY spectrum to the methine proton at 1.38 ppm and additionally to a resonance at 1.16 ppm. These correlations finally assigned the hydroxyl of one of the analogues in the second *m/z* 374 isolate to C-15 and assigned the 1.16 ppm proton to H-14, because the 1.16 ppm proton would correspond to H-18 if the hydroxyl were at C-17. H-18 can be accessed from the terminal H-20 in the HMBC and HSQC-TOCSY spectra ($^{3}J_{H-CH}$). The assignment of the remaining moiety was achieved by direct comparison with the spectra and coupling environments of **7**. Thus, the data provide good evidence that one of the analogues in the second *m/z* 374 isolate is 2-amino-12,16-dimethylicosane-3,10,15-triol (**9a**) (Figure 2).

The assignment of the third *m/z* 374 analogue was complicated because of a lack of correlations for key resonances. Nevertheless, the observable differences from **9a** were limited to only a few resonances: a different chemical shift for a C*H*OH-methine group and the shift of the C-/H-16 methine relative to **9a**, as well as the observation of a pair of resonances attributable to diastereotopic protons in the HSQC at chemical shifts similar to C-/H-15 in **7**, suggests that the third of the *m/z* 374 compounds is 2-amino-12,16-dimethylicosane-3,10,17-triol (**9b**).

Precursor Feeding Assays and Fumonisin Biosynthesis. In precursor feeding studies in which the *F. verticillioides fum1* mutant was grown in the presence of **7** (*m/z* 358), fumonisins B_1 (**1**) and B_3 (**3**) were detected in the cultures after 1 and 2 weeks of incubation (Figure 6). The formation of **1** and **3** coincided with a decline in the level of **7**. Fumonisins B_2 (**2**) and B_4 (**4**) were not detected in the same cultures after 1 and 2 weeks of incubation. When the *fum1* mutant was grown in the presence of **8**, no fumonisins were detected after 1 or 2 weeks of incubation. In addition, none of the fumonisin analogues were detected when **7** or **8** was incubated in the growth medium in the absence of the *fum1* mutant or when the mutant was grown in the absence of the metabolites. These results

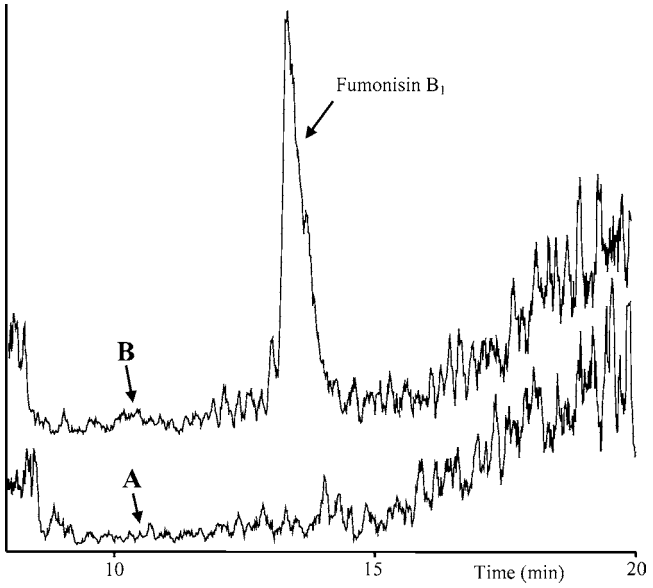

Figure 6. Precursor feeding assay with 2-amino-12,16-dimethylicosane-3,10-diol (**3**) and the *Fusarium verticillioides fum1* mutant strain GFA2364. Traces are derived from LC-MS/MS analysis: (A) GFA2364 culture without **7**; (B) GFA2364 culture to which **7** was added.

indicate that **7**, but not **8**, was transformed to **1** and **3** by the *fum1* mutant. Transformation of **7** to fumonisins supports the previously proposed hypothesis that the Fum6 monooxygenase catalyzes C-14 and C-15 hydroxylation of the fumonisin backbone.[14,18] *α,β*-Hydroxylation of carbons by cytochrome P450 monooxygenases is not uncommon in natural product biosynthesis. For example, *TRI1* and *TRI4* encode monooxygenases that catalyze hydroxylation of adjacent carbon atoms during biosynthesis of trichothecenes.[28,29] Transformation to **1** and **3** but not to **2** and **4** is consistent with the presence of a hydroxyl group at C-10 in **7**, because **1** and **3** have a C-10 hydroxyl, but **2** and **4** do not.

Our results combined with previously reported fumonisin profiles indicate that the Fum6 enzyme can utilize multiple substrates for C-14 and C-15 hydroxylation. Wild-type strains and *fum2* mutants of *F. verticillioides* produce fumonisin analogues (**2** and **4**) that lack a C-10 hydroxyl but have the C-14 and C-15 oxygen atoms as part of TCA moieties.[23] This indicates that a fumonisin-like metabolite lacking a C-10 hydroxyl can also serve as a substrate for the Fum6 enzyme. Likewise, *fum13* mutants of *F. verticillioides* produce 3-keto fumonisin analogues that have C-14 and C-15 TCA moieties.[30] This indicates that a 3-keto fumonisin-like metabolite can also serve as a substrate for Fum6. Thus, **5**, which lacks a C-10 hydroxyl, and **6**, which has a C-3 keto function, can probably also serve as substrates for Fum6.

There is evidence that several other fumonisin biosynthetic enzymes can also utilize multiple intermediates as substrates.[15,16,30,31] Thus, the current and previous studies indicate that in fumonisin biosynthesis the order of C-14/C-15 hydroxylation and esterification, C-3 keto reduction, and C-10 hydroxylation is not fixed (Figure 7). Instead, these reactions can occur either before or after one another, with the obvious exception that C-14/C-15 hydroxylation must occur before C-14/C-15 esterification (Figure 7). Furthermore, the lack of evidence for production of C-5 hydroxylated fumonisin-like metabolites by the *fum6* mutants provides

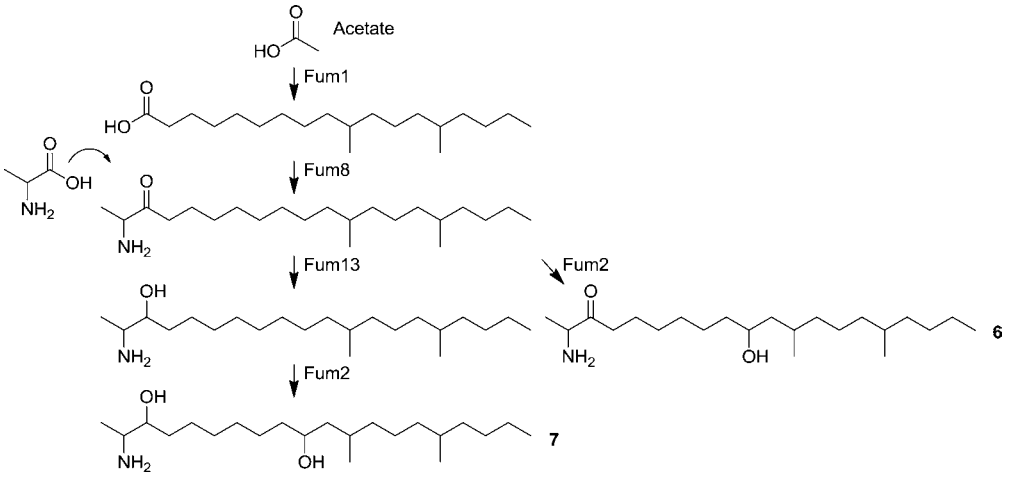

Figure 7. Truncated fumonisin biosynthetic pathway leading to formation of 2-amino-10-hydroxy-12,16-dimethylicosane-3-one (6) and 2-amino-12,16-dimethylicosane-3,10-diol (7) in *fum6* mutants of *Fusarium verticillioides*.

further evidence that, with the exception of C-10 hydroxylation, all other fumonisin biosynthetic reactions must occur prior to C-5 hydroxylation.[11,16,30,32]

The lack of transformation of **8** to fumonisins indicates that it is not a fumonisin biosynthetic intermediate. Production of metabolites that are structurally related to biosynthetic intermediates but cannot be transformed further has been reported previously for other strains of *Fusarium* carrying mutations in secondary metabolite biosynthetic genes.[15,33] These metabolites are likely artifacts formed when biosynthetic intermediates that do not normally accumulate in a cell build up when a pathway is blocked. When such intermediates accumulate, they have the potential to serve as substrates for enzymes that are not normally part of a biosynthetic pathway or for pathway enzymes that normally act on other intermediates. That **8** was not transformed to fumonisins suggests that the C-16 hydroxyl renders the fumonisin backbone an unsuitable substrate for subsequent fumonisin biosynthetic enzymes.

The presence of hydroxyl functions at C-16, C-17, and C-15 but not C-14 of compounds **8**, **9b**, and **9a**, respectively, are unique among all fumonisin-like metabolites and fumonisin analogues reported for *Fusarium*, *Aspergillus*, and *Tolypocladium*. Further analysis of the interactions of **7** and **8** with Fum6 could provide insight into the enzymatic mechanism by which the C-14 and C-15 hydroxyls are formed. Furthermore, analysis of the Fum6−**8** interaction may provide insight into whether **8** can interfere with the ability of Fum6 to catalyze C-14 and C-15 hydroxylation of metabolites that normally serve as substrates for the enzyme. Such insight could in turn provide information on how to block formation of fumonisins early in the biosynthetic process to prevent fumonisin accumulation in *F. verticillioides*-infected maize.

Although previous studies have provided insight into the fumonisin biosynthetic pathway, the earliest predicted pathway intermediates were not purified and subjected to structural analysis. In the current study, we purified and analyzed by mass spectrometry and NMR multiple compounds that accumulate in *F. verticillioides fum6* mutants. The results confirm the existence of two metabolites (**5** and **7**) previously proposed on the basis of mass spectroscopic analysis of extracts resulting when *fum1* and *fum6* mutants were cultured together.[14] Thus, our results support the hypothesis that Fum6 catalyzes fumonisin C-14 and C-15 hydroxylation and provide direct evidence for structures of early intermediates in fumonisin biosynthesis.

AUTHOR INFORMATION

Corresponding Author

*Phone: +47 23 21 62 64. Fax: +47 23 21 62 01. E-mail: silvio.uhlig@vetinst.no.

Notes

The authors declare no competing financial interest.

ACKNOWLEDGMENTS

We thank Marcie L. Moore for her technical contributions to this study.

REFERENCES

(1) Månsson, M.; Klejnstrup, M. L.; Phipps, R. K.; Nielsen, K. F.; Frisvad, J. C.; Gotfredsen, C. H.; Larsen, T. O. Isolation and NMR characterization of fumonisin B_2 and a new fumonisin B_6 from *Aspergillus niger*. *J. Agric. Food Chem.* **2010**, *58*, 949−953.

(2) Mogensen, J. M.; Frisvad, J. C.; Thrane, U.; Nielsen, K. F. Production of fumonisin B_2 and B_4 by *Aspergillus niger* on grapes and raisins. *J. Agric. Food Chem.* **2010**, *58*, 954−958.

(3) Munkvold, G. P.; Desjardins, A. E. Fumonisins in maize − can we reduce their occurrence? *Plant Dis.* **1997**, *81*, 556−565.

(4) Abbas, H. K.; Cartwright, R. D.; Shier, W. T.; Abouzied, M. M.; Bird, C. B.; Rice, L. G.; Ross, P. F.; Sciumbato, G. L.; Meredith, F. I. Natural occurrence of fumonisins in rice with *Fusarium* sheath rot disease. *Plant Dis.* **1998**, *82*, 22−25.

(5) Logrieco, A.; Doko, B.; Moretti, A.; Frisullo, S.; Visconti, A. Occurrence of fumonisin B_1 and B_2 in *Fusarium proliferatum* infected asparagus plants. *J. Agric. Food Chem.* **1998**, *46*, 5201−5204.

(6) Logrieco, A.; Ferracane, R.; Haidukowsky, M.; Cozzi, G.; Visconti, A.; Ritieni, A. Fumonisin B_2 production by *Aspergillus niger* from grapes and natural occurrence in must. *Food Addit. Contam. Part A: Chem. Anal. Control Expo. Risk Assess.* **2009**, *26*, 1495−1500.

(7) Varga, J.; Kocsube, S.; Suri, K.; Szigeti, G.; Szekeres, A.; Varga, M.; Toth, B.; Bartok, T. Fumonisin contamination and fumonisin producing black Aspergilli in dried vine fruits of different origin. *Int. J. Food Microbiol.* **2010**, *143*, 143−149.

(8) Howard, P. C.; Eppley, R. M.; Stack, M. E.; Warbritton, A.; Voss, K. A.; Lorentzen, R. J.; Kovach, R. M.; Bucci, T. J. Fumonisin B_1 carcinogenicity in a two-year feeding study using F344 rats and B6C3F(1) mice. *Environ. Health Perspect.* **2001**, *109*, 277−282.

(9) Marasas, W. F. O.; Riley, R. T.; Hendricks, K. A.; Stevens, V. L.; Sadler, T. W.; Gelineau-van Waes, J.; Missmer, S. A.; Cabrera, J.;

Torres, O.; Gelderblom, W. C. A.; Allegood, J.; Martinez, C.; Maddox, J.; Miller, J. D.; Starr, L.; Sullards, M. C.; Roman, A. V.; Voss, K. A.; Wang, E.; Merrill, A. H. Fumonisins disrupt sphingolipid metabolism, folate transport, and neural tube development in embryo culture and *in vivo*: a potential risk factor for human neural tube defects among populations consuming fumonisin-contaminated maize. *J. Nutr.* **2004**, *134*, 711−716.

(10) Bezuidenhout, S. C.; Gelderblom, W. C. A.; Gorstallman, C. P.; Horak, R. M.; Marasas, W. F. O.; Spiteller, G.; Vleggaar, R. Structure elucidation of the fumonisins, mycotoxins from *Fusarium moniliforme*. *J. Chem. Soc., Chem. Commun.* **1988**, *11*, 743−745.

(11) Alexander, N. J.; Proctor, R. H.; McCormick, S. P. Genes, gene clusters, and biosynthesis of trichothecenes and fumonisins in *Fusarium*. *Toxin Rev.* **2009**, *28*, 198−215.

(12) Du, L.; Zhu, X.; Gerber, R.; Huffman, J.; Lou, L.; Jorgenson, J.; Yu, F.; Zaleta-Rivera, K.; Wang, Q. Biosynthesis of sphinganine-analog mycotoxins. *J. Ind. Microbiol. Biotechnol.* **2008**, *35*, 455−464.

(13) Gerber, R.; Lou, L. L.; Du, L. C. A PLP-dependent polyketide chain releasing mechanism in the biosynthesis of mycotoxin fumonisins in *Fusarium verticillioides*. *J. Am. Chem. Soc.* **2009**, *131*, 3148−3149.

(14) Bojja, R. S.; Cerny, R. L.; Proctor, R. H.; Du, L. C. Determining the biosynthetic sequence in the early steps the fumonisin pathway by use of three gene-disruption mutants of *Fusarium verticillioides*. *J. Agric. Food Chem.* **2004**, *52*, 2855−2860.

(15) Butchko, R. A. E.; Plattner, R. D.; Proctor, R. H. Deletion analysis of *FUM* genes involved in tricarballylic ester formation during fumonisin biosynthesis. *J. Agric. Food Chem.* **2006**, *54*, 9398−9404.

(16) Zaleta-Rivera, K.; Xu, C. P.; Yu, F. G.; Butchko, R. A. E.; Proctor, R. H.; Hidalgo-Lara, M. E.; Raza, A.; Dussault, P. H.; Du, L. C. A bidomain nonribosomal peptide synthetase encoded by *FUM14* catalyzes the formation of tricarballylic esters in the biosynthesis of fumonisins. *Biochemistry* **2006**, *45*, 2561−2569.

(17) Proctor, R. H.; Desjardins, A. E.; Plattner, R. D.; Hohn, T. M. A polyketide synthase gene required for biosynthesis of fumonisin mycotoxins in *Gibberella fujikuroi* mating population A. *Fungal Genet. Biol.* **1999**, *27*, 100−112.

(18) Proctor, R. H.; Busman, M.; Seo, J. A.; Lee, Y. W.; Plattner, R. D. A fumonisin biosynthetic gene cluster in *Fusarium oxysporum* strain O-1890 and the genetic basis for B versus C fumonisin production. *Fungal Genet. Biol.* **2008**, *45*, 1016−1026.

(19) Seo, J. A.; Proctor, R. H.; Plattner, R. D. Characterization of four clustered and coregulated genes associated with fumonisin biosynthesis in *Fusarium verticillioides*. *Fungal Genet. Biol.* **2001**, *34*, 155−165.

(20) Tuite, J. *Plant Pathological Methods: Fungi and Bacteria*; Burgess Publishing: Minneapolis, MN, 1969.

(21) Plattner, R. D.; Shackelford, D. D. Biosynthesis of labeled fumonisins in liquid cultures of *Fusarium moniliforme*. *Mycopathologia* **1992**, *117*, 17−22.

(22) Plattner, R. D.; Weisleder, D.; Poling, S. M. Analytical determination of fumonisins and other metabolites produced by *Fusarium moniliforme* and related species on corn. In *Fumonisins in Food*; Jackson, L. S., DeVries, J. W., Bullerman, L. B., Eds.; Plenum Press: New York, 1996.

(23) Proctor, R. H.; Plattner, R. D.; Desjardins, A. E.; Busman, M.; Butchko, R. A. E. Fumonisin production in the maize pathogen *Fusarium verticillioides*: genetic basis of naturally occurring chemical variation. *J. Agric. Food Chem.* **2006**, *54*, 2424−2430.

(24) Uhlig, S.; Petersen, D.; Flåøyen, A.; Wilkins, A. L. 2-Amino-14,16-dimethyloctadecan-3-ol, a new sphingosine analogue toxin in the fungal genus *Fusarium*. *Toxicon* **2005**, *46*, 513−522.

(25) Branham, B. E.; Plattner, R. D. Alanine is a precursor in the biosynthesis of fumonisin B_1 by *Fusarium moniliforme*. *Mycopathologia* **1993**, *124*, 99−104.

(26) Richards, S. A.; Hollerton, J. C. *Essential Practical NMR for Organic Chemistry*; Wiley: Chichester, West Sussex, UK, 2011.

(27) Maume, B. Gas chromatographic and mass spectrometric study of trimethylsilyl ethers of cardic aglycones. *Anal. Lett.* **1968**, *1*, 401−415.

(28) McCormick, S. P.; Alexander, N. J.; Proctor, R. H. *Fusarium Tri4* encodes a multifunctional oxygenase required for trichothecene biosynthesis. *Can. J. Micribiol.* **2006**, *52*, 636−642.

(29) McCormick, S. P.; Harris, L. J.; Alexander, N. J.; Ouellet, T.; Saparno, A.; Allard, S.; Desjardins, A. E. Tri1 in *Fusarium* encodes a P450 oxygenase. *Appl. Environ. Microbiol.* **2004**, *70*, 2044−2051.

(30) Butchko, R. A. E.; Plattner, R. D.; Proctor, R. H. *FUM13* encodes a short chain dehydrogenase/reductase required for C-3 carbonyl reduction during fumonisin biosynthesis in *Gibberella moniliformis*. *J. Agric. Food Chem.* **2003**, *51*, 3000−3006.

(31) Yi, H.; Bojja, R. S.; Fu, J.; Du, L. C. Direct evidence for the function of *FUM13* in 3-ketoreduction of mycotoxin fumonisins in *Fusarium verticillioides*. *J. Agric. Food Chem.* **2005**, *53*, 5456−5460.

(32) Ding, Y.; Bojja, R. S.; Du, L. C. Fum3p, a 2-ketoglutarate-dependent dioxygenase required for C-5 hydroxylation of fumonisins in *Fusarium verticillioides*. *Appl. Environ. Microbiol.* **2004**, *70*, 1931−1934.

(33) McCormick, S. P.; Taylor, S. L.; Plattner, R. D.; Beremand, M. N. Bioconversion of possible T-2 toxin precursors by a mutant strain of *Fusarium sporotrichioides* NRRL 3299. *Appl. Environ. Microbiol.* **1990**, *6*, 702−706.